Wind and Structures, *Vol. 27, No. 6 (2018) 357-368*
DOI: https://doi.org/10.12989/was.2018.27.6.357

Long-term monitoring of super-long stay cables on a cable-stayed bridge

Xiang Shen, Ru-jin Ma*, Chun-xi Ge and Xiao-hong Hu

Department of Bridge Engineering, Tongji University, 1239 Siping Road Shanghai, China

(Received May 5, 2018, Revised October 3, 2018, Accepted October 11, 2018)

Abstract. For a long cable-stayed bridge, stay cables are its most important load-carrying components. In this paper, long-term monitoring of super-long stay cables of Sutong Bridge is introduced. A comprehensive data analysis procedure is presented, in which time domain and frequency domain based analyses are carried out. In time domain, the vibration data of several long stay cables are firstly analyzed and the standard deviation of the acceleration of stay cables, and its variation with time are obtained, as well as the relationship between in-plane vibration and out-plane vibration. Meanwhile, some vibrations such as wind and rain induced vibration are detected. Through frequency domain analysis, the basic frequencies of the stay cables are identified. Furthermore, the axial forces and their statistical parameters are acquired. To investigate the vibration deflection, an FFT-based decomposition method is used to get the modal deflection. In the end, the relationship between the vibration amplitude of stay cables and the wind speed is investigated based on correlation analysis. Through the adopted procedure, some structural parameters of the stay cables have been derived, which can be used for evaluating the component performance and corresponding management of stay cables.

Keywords: stay cable; long-term monitoring; vibration; axial force; FFT-based decomposition method

1. Introduction

Stay cables, with superior structural performance and elegant appearance, make them widely used in bridges, gymnasia, coastal engineering, etc. However, inclined cables on cable-stayed bridges are easily excited by wind action due to their low structural damping (Chen *et al*. 2016, Raftoyiannis and Michaltsos 2016, Wu *et al.* 2016). Therefore, it has been reported that a lot of stay cables on full-scale bridges showed various wind-induced vibration risks such as non-linear free vibrations (Schemmann and Smith 2015, Sun and Zhao *et al.* 2015) and forced vibrations (Sardesai and Desai 2014, Sardesai and Desai 2014), which will threaten the service life of such bridges (Main and Jones 1999). Stallings investigated the fatigue behavior of stay cables and found the fatigue life of a stay-cable (Stallings and Frank 1991). Wang gave advice on stay-cable maintenance and replacement (Wang *et al.* 2012). Zhang overcame the limitations of the small displacement hypothesis and developed a new method to identify parameters relating to resonance in stay cables (Zhang and Peil 1999). Hikami showed the influence of water rivulets tracking along the cable (Hikami and Shiraishi 1988). Zuo conducted field observations to show the similarities and differences between vortex-induced vibration and rain-wind-induced vibration (Zuo *et al.* 2008).

However, for the sake of the long-term performance and maintenance of stay cables, more practical methods should be proposed. Structural health monitoring systems (SHMS) have been widely employed to understand structural performance (Kudva 1994), with the purpose of obtaining the actual behavior of stay cables. A lot of work has been conducted in this area. Wang combined SHMS and finite element strain data to assess the fatigue reliability index of girder components in a long-span cable-stayed bridge (Wang *et al.* 2010). Lu proposed an approach with which to detect bridge damage (Lu 2008), whose basic idea is that the response of a normal structure differs from that of a damaged structure. Follen proposed a robust and computationally efficient method for bridge damage detection, using only measured strain data from truck loading events (Follen *et al.* 2014). Mao presented a structural transmissibility measurement-based approach for system damage detection (Mao and Todd 2010). Deng investigated the fatigue performance of welded details on the Runyang Bridge based on SHMS data (Deng *et al.* 2015).

Even though a lot of research has been conducted based on analysis of monitoring data, most studies were based on short-term monitoring. Furthermore, there has been a lack of long-term research on stay cables, especially under complex service environment. Because of variability of the stiffness of stay cables, identification of their parameters is a time-consuming and laborious process. To solve this problem, an automatic algorithm to identify the base modal frequency of stay cables is proposed. Then vibration amplitude and tension force of stay cables are analyzed on the basis of the identified base model vibration frequency. This paper presents a long-term monitoring study and evaluation procedures as follows. Firstly, the SHMS of Sutong Bridge is briefly introduced. Secondly, from the aspects of both the time domain and frequency domain, stay cable tension force, vibration amplitude, and the

*Corresponding author, Ph.D., Associate Professor
E-mail: rjma@tongji.edu.cn

http://www.techno-press.com/journals/was&subpage=7 ISSN: 1226-6116 (Print), 1598-6225 (Online)

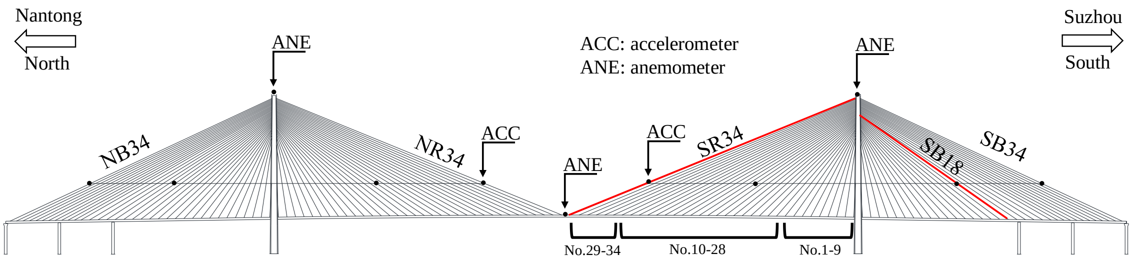

Fig. 1 Layout of sensors used in the study

Table 1 Parameters of stay cables of SR34 and SB18

	L (m)	θ (°)	L_X (m)	L_y (m)	H_a (m)	H_d (m)	$\overline{m}$ (kg/m)	Tension (KN)	Damper type	Diameter (mm)
SR34	577	23	529	229	5	4	102	7078	MRD	161
SB18	337	34	281	187	5	3.5	76	4649	HD	139

relationship between vibration and wind, as well as vibration between out-plane direction and in-plane direction, are analyzed. Finally, some threshold values are deduced based on the statistics of tension force and vibration amplitude of stay cables, which can be applied into maintenance and understanding the working performance of stay cables by the maintenance crew.

2. Brief introduction to the structural monitoring system

In recent years, SHMS have been extensively applied to long-span bridges. As a long-span bridge with the longest stay cables in China, Sutong Bridge has been equipped with an SHMS. The initial objective of the system is to understand the structural performance instantly. During the past 20 years, even though SHMSs have been used to identify structural damage, the majority of collected data has always seemed useless in terms of structure management and maintenance, because the key message was always submerged by insignificant information and insufficient analysis of these data. To explain the data and make them valuable to management and maintenance, some attempts have been made to understand the performance of stay cables of Sutong Bridge.

The SHMS of Sutong Bridge consists of many sensors including anemometers, accelerometer, strain gauges, thermometers, moisture meters, etc. To interpret the vibration data of stay cables, two kinds of data such as acceleration of stay cables and wind speed are used. There are 272 stay cables whose length ranges from 153 m to 577 m in Sutong Bridge. To suppress the excessive vibration of these stay cables, different strategies were applied to these cables with different lengths. For those long stay cables such as No. 29 to No. 34, as seen in Fig. 1, magnetorheological dampers (MRD) were installed. For those medium long stay cables such as No.10 to No.28, hydraulic dampers (HD) were installed. For those short stay cables, such as No.1 to No.9, no external dampers were installed. Considering the different strategies, two types of long stay cables, i.e., SR34 and SB18, as shown in Fig. 1, are chosen for observation. Here ‘S’ denotes the stay cables located on the south part of the bridge, while ‘R’ and ‘B’ denote the stay cables close to the river and the bank respectively. These two stay cables also represent cables are equipped with the MRD and HD, respectively. Both of the stay cables belong to the west-side stay-cable plane. For all those monitored stay cables, two accelerometers were installed at the same position of each stay cable to record in-plane and out-plane vibrations. The sampling frequency of the accelerometers was set to be 20 Hz. The installing position of accelerometers and the dampers are given in Fig. 2. Table 1 also gives the parameters of stay cables of SR34 and SB18. Besides the accelerometers, four anemometers with two on the top of both pylons and the others on the deck at the mid-span, were also installed on the Sutong Bridge.

3. Performance evaluation procedure

In this paper, the variation of tension force and the vibration amplitude of stay cables are focused which can directly reflect the working performance. Time domain analysis and frequency domain analysis are both carried out to obtain such parameters as tension force, vibration amplitude, and vibration acceleration. In the time domain, the root mean square (RMS) vibration acceleration is calculated. Based on their tendency of long term variation, abnormal and excessive vibrations can be discerned. However, the acceleration alone cannot reflect the working performance, since all vibration modes are mixed up and higher modes always contribute more to the vibration acceleration but less to the vibration amplitude. As a result, acceleration data need to be translated into some modal combination to calculate the vibration amplitude. Therefore, a frequency domain method is used to find the modal

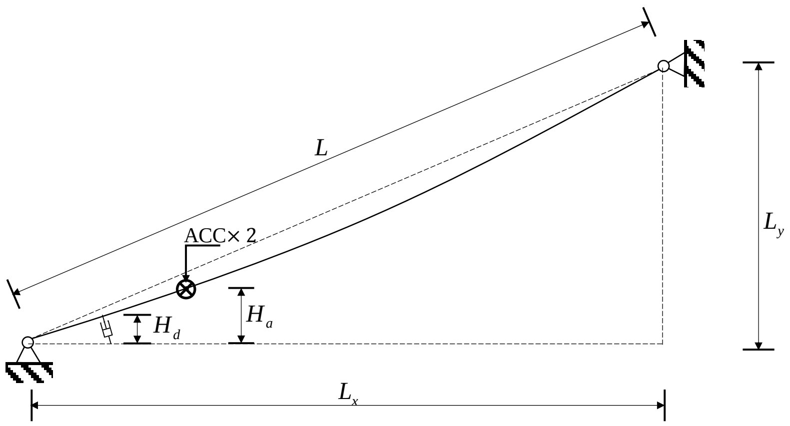

Fig. 2 Layout of the accelerometers and dampers on SR34 and SB18

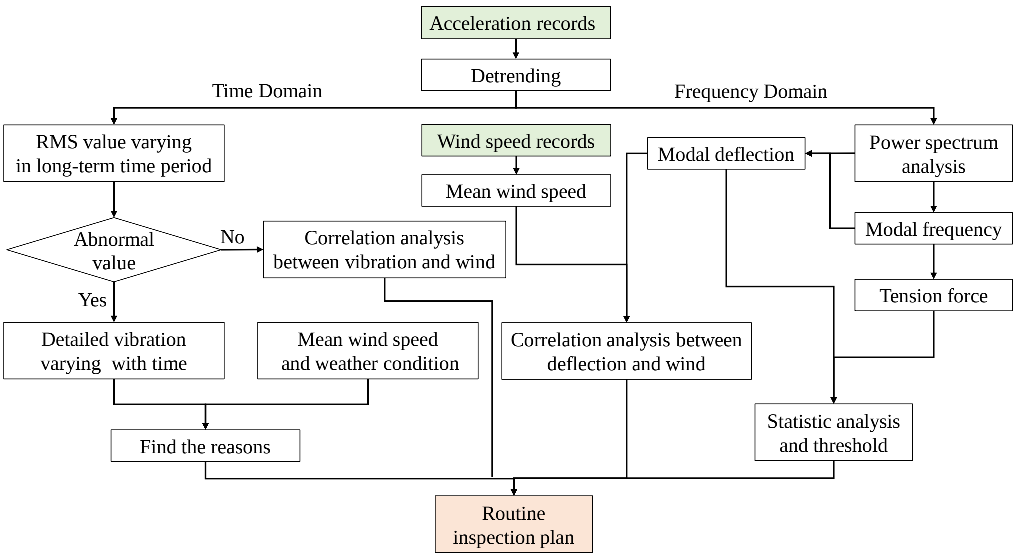

Fig. 3 Flow chart of performance evaluation procedure for stay cables

vibration amplitudes and tension forces of stay cables. To discover the relationship between vibration and wind excitation, correlation analysis is performed to discover the actual performance of stay cables under different wind speed. Statistical analysis of tension force directly allows the assessment of the normal range of tension force of the stay cables. Finally, limiting values are given to evaluate the performance of stay cables. The performance evaluation procedure of stay cables is shown in Fig. 3.

4. Time domain based performance evaluation procedure

4.1 Statistical analysis of acceleration

Time domain statistical analysis of vibration was firstly conducted over a long-term period because of its intuitional feature and easy understandability. To get the statistical values of vibration, the RMS vibration acceleration in every 10 minutes was calculated. 144 vibration acceleration RMS values of one accelerometer can be generated every day. For simplicity, two stay cables, SB18 and SR34, are focused on here. In this paper, the data from May, 2012 to December, 2012 are utilized.

The daily maximum RMS of the acceleration as a function of the time is plotted in Fig. 4. In-plane vibration and out-plane vibration of two stay cables are given separately. For cable SR34, vibration in in-plane and out-plane directions remained relatively steady in one year. The maximum RMS of vibration acceleration in the in-plane direction and out-plane direction were 0.3 m/s^2 and 0.22 m/s^2 respectively. For cable SB18, RMS of vibration accelerations in the out-plane direction were smaller than those in the in-plane direction. Due to the meteorological conditions at the bridge site, the wind speed is stronger in

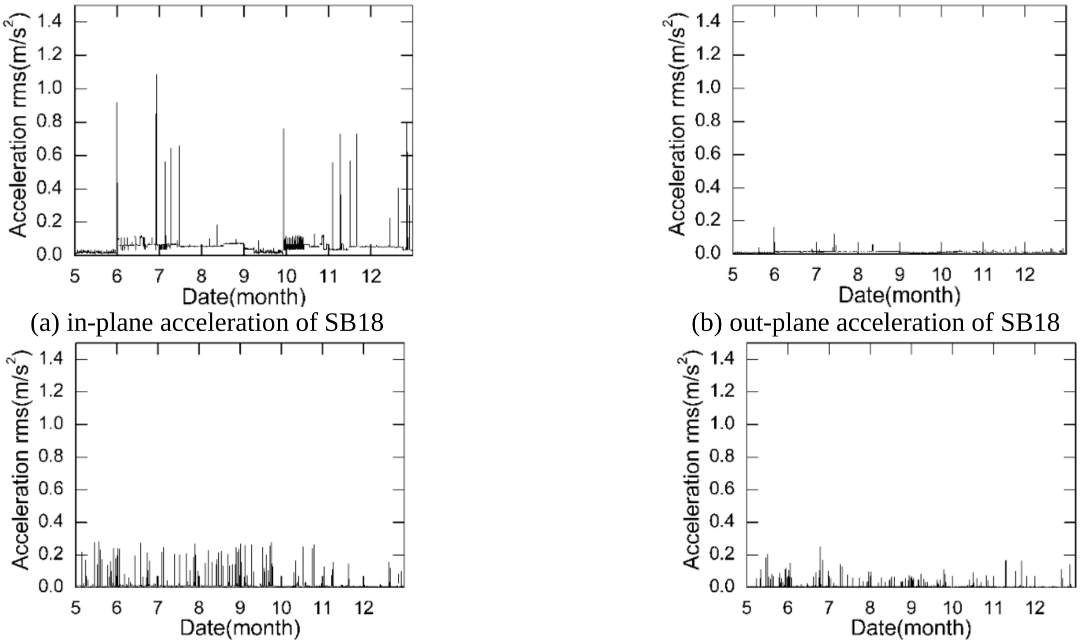

(a) in-plane acceleration of SB18 (b) out-plane acceleration of SB18

(c) in-plane acceleration of SR34 (d) out-plane acceleration of SR34

Fig. 4 RMS of vibration acceleration varying with time

summer and winter than in spring and autumn. As a result, the vibration intensity is higher in summer and winter. The acceleration RMS of SB18 in the in-plane direction can reach 1.1 m/s^2. From Fig. 4, it is clear that at some time, the RMS of acceleration deviates from its normal value. It is meaningful to further investigate the data at those abnormal times.

4.2 Abnormity analysis of strong vibration in time domain

To obtain more detailed information about the acceleration at these abnormal vibration, two short duration, i.e., 1h and 6s, are plotted in Fig. 5. The one-hour-long pictures are used to highlight the strong vibration period and the 6s section of vibration records can explain the strong vibration in detail. Taking Fig. 5(b) as an example, at 05:00AM on 21 June, cable SB18 vibrated severely. According to the data collected by anemometers on the bridge, the wind speed was about 5.7 m/s. A certain type of wind-induced vibration must happen at that time, but vortex-induced vibration mechanisms can be excluded because for the stay-cable structure, the Strouhal number is around 0.2, which means that the wind speed leading to vortex-induced vibration is less than 3 m/s (Matsumoto *et al.* 2001). After the confirmation of rainfall from the meteorological station, the vibration can be similarly regarded as wind-rain vibration.

4.3 Correlation analysis between in-plane and out-plane vibration

To reveal the type of vibration in the in-plane and out-plane directions, correlation analysis was carried out. The results are plotted in Fig. 6. For SB18, two types of vibrations can be identified. Both of them are dominated by the in-plane vibration. It can be concluded that SB18 mainly suffered from in-plane vibration. For SR34, two types of vibrations can also be discerned. Different from SB18, SR34 has two different types of vibration, with one dominated by in-plane vibration and the other by out-plane vibration. Vibration intensity and their probability of occurrence are also calculated. After statistical analysis, it is found that the special vibration occurred when the RMS of acceleration of SB18 and SR34 is greater than 0.1 m/s^2 and 0.02 m/s^2 respectively. Therefore, the discriminant thresholds of abnormal vibration for SB18 and SR34 are set as 0.1 m/s^2 and 0.02 m/s^2 respectively. Through statistical analysis of the special vibration, it can also be found that vibration types 1 and 2 account for 2.6% and 0.3% for SB18, while vibration types 1 and 2 account for 3.6% and 0.6% for SR34.

4.4 Correlation analysis between vibration acceleration and wind speed

It has been reported that many stay cables show various types of wind-induced vibration, such as galloping and vortex-induced vibration. In this research, to discover the relationship between the vibration acceleration and wind speed, correlation analysis was carried out, as seen in Figs. 7 and 8, which gives the RMS values of acceleration varying with 10-minute averaged wind speeds. It can be seen that strong vibration happened within wind speeds ranging from 6 m/s to 12 m/s. To further investigate the vibration mechanism, detailed analysis in frequency domain will be given in the following section.

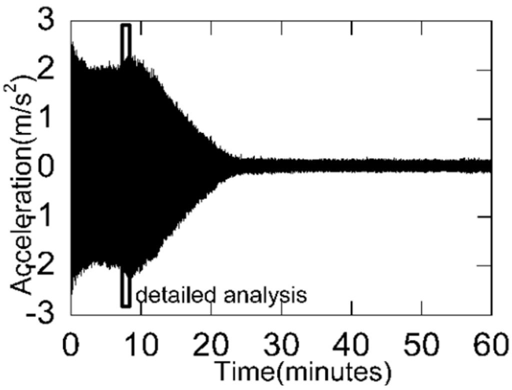

(a) in-plane of SB18(wind speed 5.2 m/s)

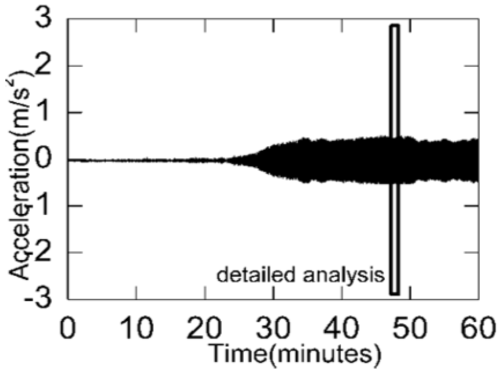

(b) in-plane of SR34(wind speed 5.7 m/s)

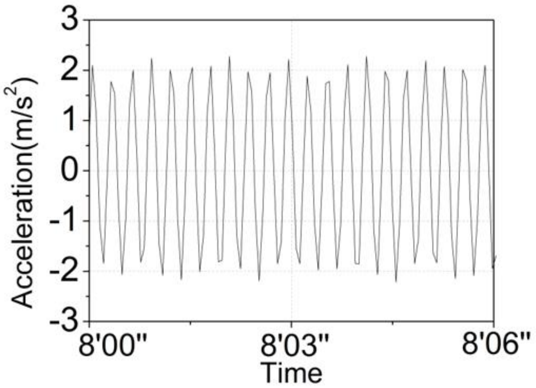

(c) detailed vibration of SB18

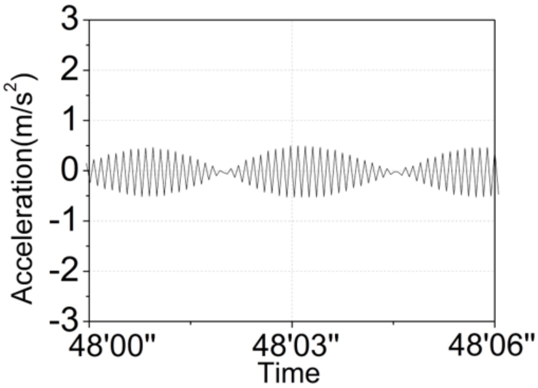

(d) detailed vibration of SR34

Fig. 5 Vibration acceleration in detail

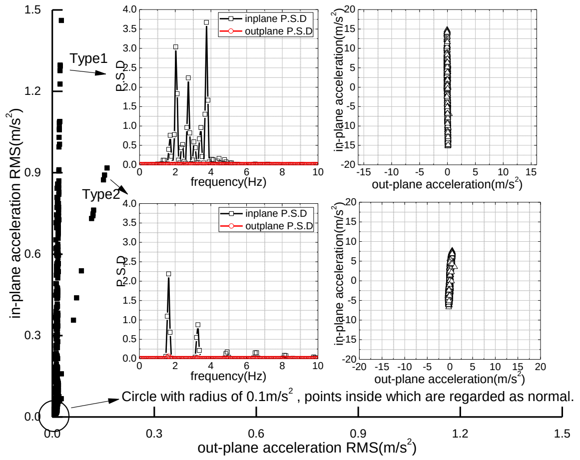

(a) SB18

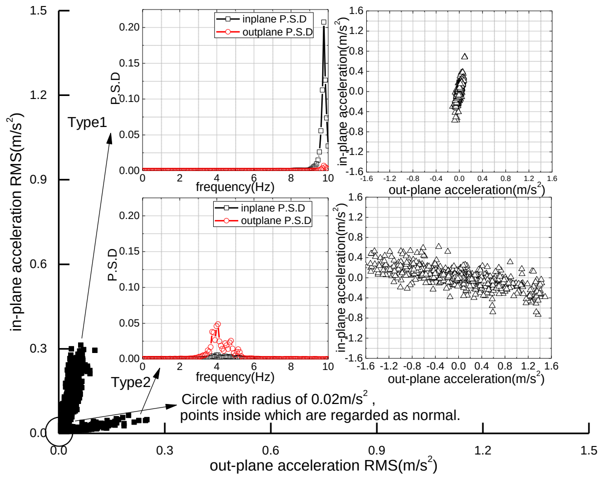

(b) SR34

Fig. 6 Relationship between in-plane and out-plane vibration

5. Frequency domain based analysis on the vibration of stay cables

5.1 Frequency domain analysis of vibration

The actual stay-cable vibration consists of a series of vibrations at different frequencies. To study each modal vibration at different frequencies, FFT based analysis is used because the power spectrum from the FFT method has provide a different frequency perspective with which vibration mechanism can be better understood. Three samples of SR34 in the time domain, and their power spectra at different wind speeds, are shown in Figs. 9 and 10, separately.

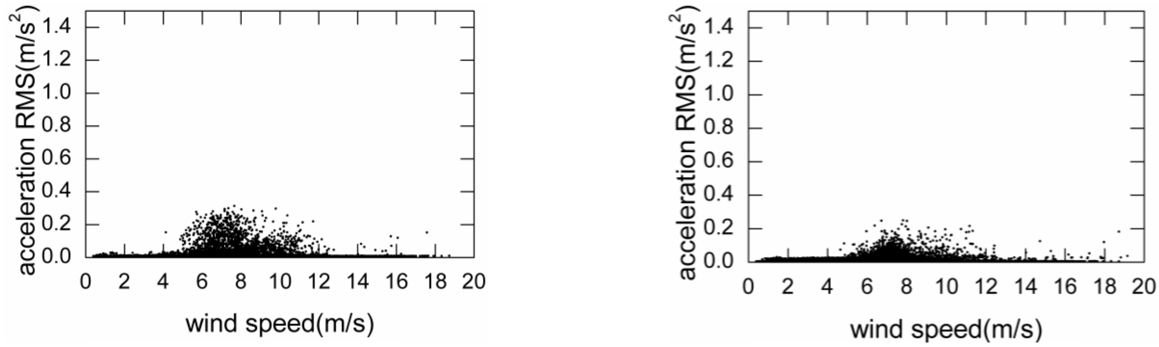

(a) in-plane vibration of SR34 (b) out-plane vibration of SR34

Fig. 7 Acceleration RMS of SR34 vs mean wind speed

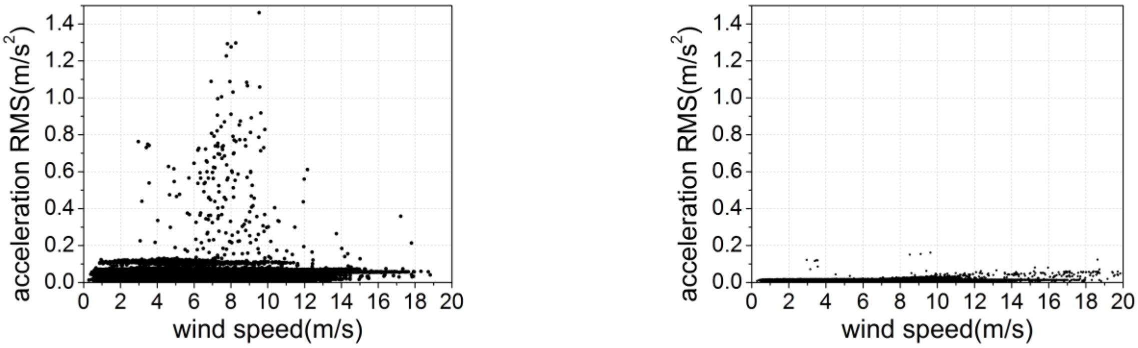

(a) in-plane vibration of SB18 (b) out-plane vibration of SB18

Fig. 8 Acceleration RMS of SB18 vs mean wind speed

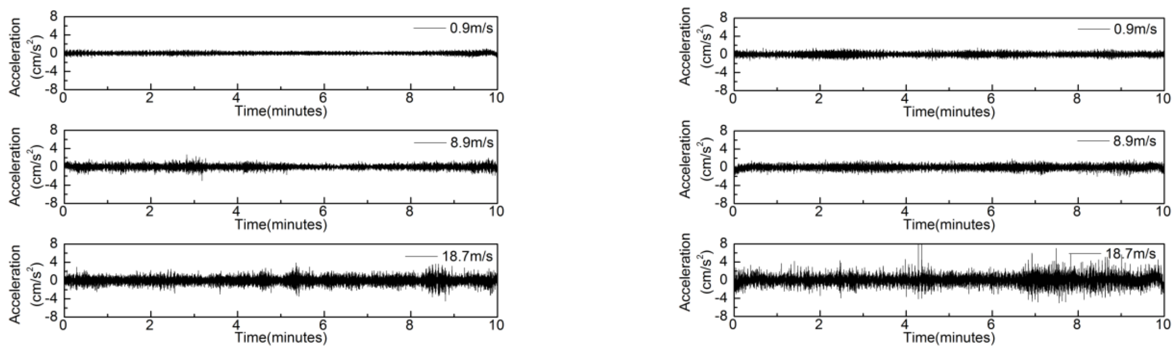

(a) in-plane vibration (b) out-plane vibration

Fig. 9 Time history acceleration of SR34

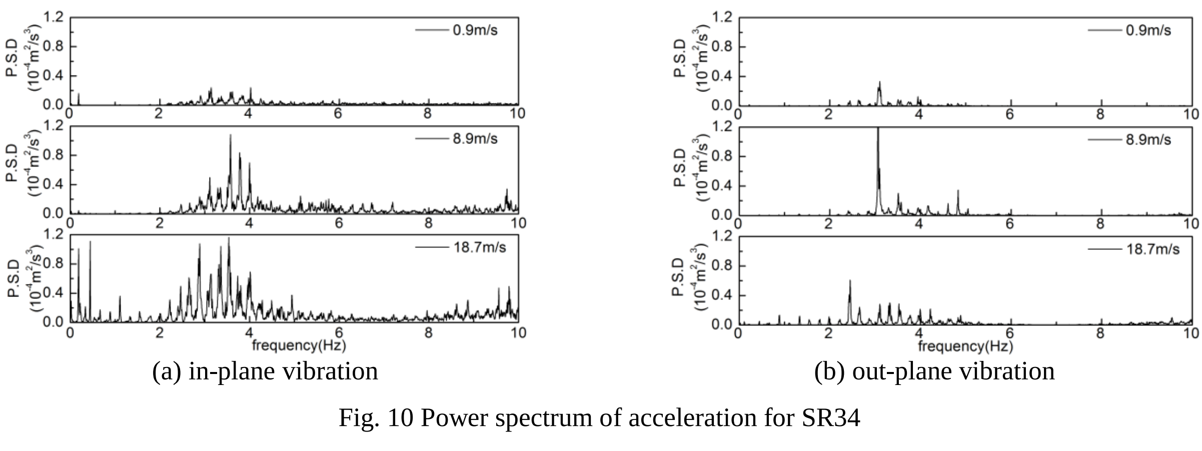

(a) in-plane vibration (b) out-plane vibration

Fig. 10 Power spectrum of acceleration for SR34

From Fig. 9, two tendencies for in-plane and out-plane vibration can be found. For in-plane vibration, acceleration increases with the wind speed, while this trend is near-negligible for out-plane vibration. Fig. 10 focuses on the energy distribution in frequency domain. With increasing wind speed, the energy in dominant modal frequencies increases, especially for in-plane vibrations at a frequency of less than 1 Hz under strong wind, which may lead to dramatic change in stay-cable tension force and cable vibration amplitude.

5.2 A new algorithm to identify base frequency of stay cables

A lot of research has been conducted to identify the base frequency of stay cables because of its importance to understand the cable tension force. A new algorithm is proposed to automatically identify the base frequencies of stay cables. The basic hypothesis of the algorithm is based on the fact that the frequency difference between each two adjacent vibration modes should remain constant and be equal to the first mode vibration frequency or the so-called base frequency (MacDonald 2016). For vibration modes higher than the fifth mode, the frequency difference between each two adjacent vibration modes should nearly be the base frequency and the deviation is negligible. Based on the above hypothesis, the base frequency of stay cables can be obtained based on the least square method (LSM) followed by the below procedure, as shown in Fig. 11.

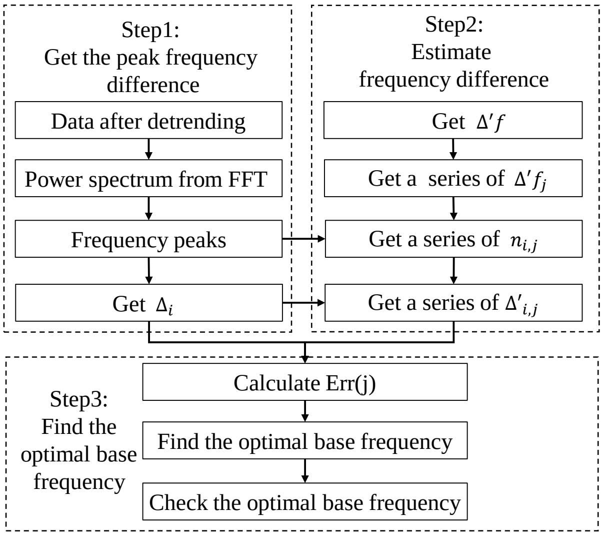

Fig. 11 Identification of base frequency of stay cables based on LSM algorithm

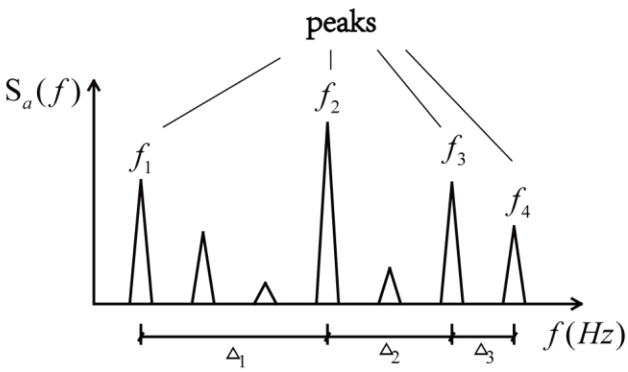

Fig. 12 Energy peaks and peak frequency differences between modal frequencies

Step 1): Get peak frequency difference

The first five or more energy peaks can be found in power spectrum of acceleration. The corresponding peak frequencies are obtained and named in sequence as f_{i}, as shown in Fig. 12. The peak differences between adjacent energy peaks can be calculated from Eq. (1)

$$\Delta_{\mathrm{i}} = f_{i+1} - f_i \tag{1}$$

where, Δ_i is the peak frequency difference between adjacent energy peaks, f_{i} is the i-th modal frequency having dominant energy.

Step 2): Estimate frequency difference

(1) Before estimating Δ'_i, the initial base frequency ($\Delta' f$) should be got, which could be calculated from the design data or tests after completion of the bridge. In this paper, the initial frequency is assigned by the identified value from acceleration data of the first day.

(2) The real-time base frequency (Δf) should be around the initial base frequency ($\Delta' f$). So a series of assumed base frequencies ($\Delta' f_{j,\, j=1,2,3...}$) are assigned with the value ranging from 0.7 $\Delta' f$ to 1.3 $\Delta' f$, with the step of 0.02 $\Delta' f$.

(3) For each f_{i} from the power spectrum, a series of mode numbers $n_{i,j}$ should be calculated based on the assumed base frequency $\Delta' f_j$ as follows

$$n_{i,j} = \frac{f_{\mathrm{i}}}{\Delta' f_j} \tag{2}$$

where $n_{i,j}$ should be rounded up and down into integer number.

(4) For each real measured Δ_{i}, a series of frequency differences $\Delta'_{i,j}$ based on $\Delta' f_j$ and $n_{i,j}$ can be calculated as follows

$$\Delta'_{i,j} = \Delta' f_j \cdot (n_{i+1,j} - n_{i,j}) \tag{3}$$

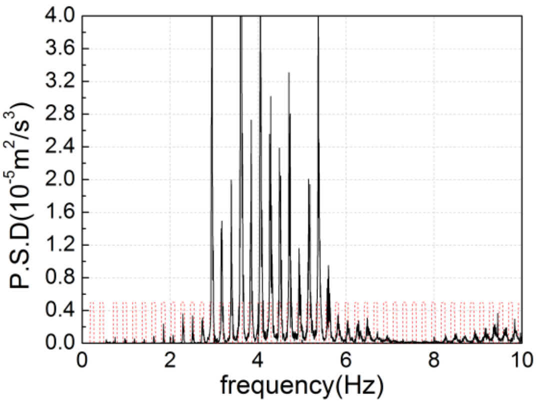

Fig. 13 Base frequency identification by LSM

Step 3): Find the optimal base frequency $\Delta f_{optimal}$

In this step, an optimal base frequency should be found to represent the real-time base frequency Δf by the least squares method (LSM) as following sub-steps.

(1) For each assumed $\Delta' f_j$, the error between Δf and $\Delta' f_j$ is noted as $Err(j)$ which is defined as Eq. (4).

$$Err(j) = \frac{\sum_{i=1}^{N}(\Delta_i - \Delta'_{i,j})^2{}_{i,j}}{N} \tag{4}$$

where N is the number of Δ_i.

(2) Find the minimum $Err(j)$, through the index j, the $\Delta' f_j$ is chosen as the optimal base frequency $\Delta f_{optimal}$, namely $\Delta f_{optimal} = \Delta' f_j$.

(3) Confirm the $\Delta f_{optimal}$: To avoid incorrect results, the value of Err_i should be checked. If $Err(j) > 0.05\Delta' f$, the result of this time section was abandoned.

By following the above procedure, a case study was analyzed. Taking the acceleration signal of SR34 from 11:10 to 11:20 pm on 16 June as an example, Fig. 13 shows the result of the LSM method. The solid lines represent the power spectrum of the acceleration, while the dashed lines represent the frequency range with frequencies of $n \times \Delta f \pm 0.08\Delta f$. It can be seen that, the frequency range based on identified base frequency from LSM coincided with the power spectrum.

5.3 Stay-cable tension force analysis

The relationship between tension force and frequency of stay cables is given by Eq. (5) (Feng *et al.* 2017)

$$H = 4L^2 \Delta f^2 \bar{m} \tag{5}$$

Table 2 Probability of tension force of stay cables

Probability of exceedance P_e	SB18		SR34	
	H_{min} (ton)	H_{max} (ton)	H_{min} (ton)	H_{max} (ton)
10^{-3}	413	452	629	689
10^{-4}	409	456	622	695
10^{-5}	405	459	617	700
10^{-6}	401	463	611	706

where H is the tension force of stay cable, L is the length of stay cable, $\bar{m}$ is the self-weight of stay cable per metre. Based on the procedure discussed above, the base frequency and the tension force were obtained.

The tension forces were calculated every 10 minutes, so 144 tension force data were collected every day. To show the changes in the tension force of stay cable throughout each day, candlestick chart was used to present the daily variation range of the tension force, as shown in Fig. 14(a). It is found that the amplitude of variation of tension force in a day was less than 40 ton. Fig. 14(b) gives the frequency statistical results of the tension force, which can be considered as a random variable obeying a Gaussian distribution, with a mean value of 658.6 tons and a standard deviation of 9.95 tons. By long period of monitoring, the probability distribution of tension force can be obtained. If different probability of exceedance of tension force are considered, the threshold value of tension force can also be determined as shown in Table 2. Take stay cable of SR34 as an example, it is suggested that when tension force higher than 700 ton or lower than 617 ton, some emergence inspections to stay cables should be carried out.

5.4 Modal vibration amplitude analysis

Excessive vibration amplitude should be prevented in a cable-stayed bridge to maintain the safety of its stay cables. However, the vibration amplitude cannot be directly obtained through acceleration-based monitoring. In this study, the power spectrum of the acceleration was translated into a power spectrum of displacement as follows

$$S_x(\omega) = \frac{S_{\ddot{x}}(\omega)}{(\omega)^4} \tag{6}$$

where， x is the displacement of the stay cable at measuring point, ω is the circular frequency, $S_x(\omega)$ is the power spectral density function of x and $S_{\ddot{x}}(\omega)$ is the power spectral density function of $\ddot{x}$.

For each modal vibration, the mean square deviation of its amplitude can be calculated by using Eq. (7)

$$\sigma_{Ai}^2 = \frac{1}{2\pi}\int_{\omega_i - 0.4\pi\Delta f}^{\omega_i + 0.4\pi\Delta f} S_x(\omega)d\omega \tag{7}$$

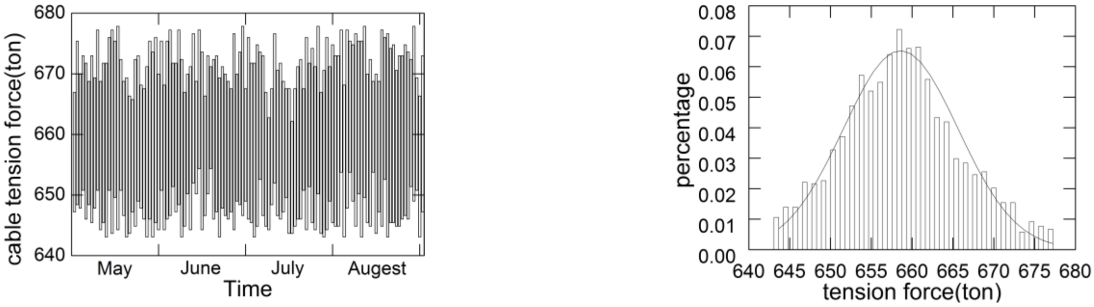

(a) Daily variation of tension force (b) Probability density distribution

Fig. 14 Daily variation of tension force and its probability distribution of stay cable SR34

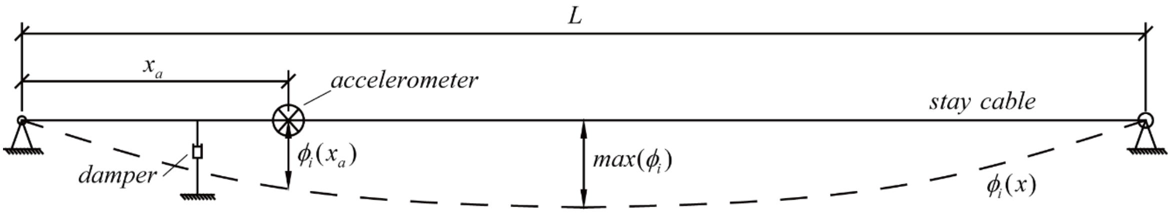

Fig. 15 Relationship of modal amplitude between gauge point and the max amplitude point

Table 3 Occurrence probability of maximum averaged modal amplitude

amplitude(m)		0~0.05	0.05~0.1	0.1~0.15	0.15~0.2	0.2~0.25
in-plane	first mode (%)	99.93	0.07	0	0	0
	second mode (%)	100	0	0	0	0
out-plane	first mode (%)	99.887	0.092	0.015	0.003	0.003
	second mode (%)	100	0	0	0	0

where σ_{Ai} is the RMS vibration amplitude at the point of accelerometer, ω_i is the i-th modal vibration circular frequency, and Δf can be obtained from the LSM. Then σ_{Ai} needs to be converted into the modal maximum amplitude.

Assuming the modal shape of stay cables as sinusoidal curve, the variance at the measurement point is given by Eq. (8)

$$\sigma_{Ai}^2 = \frac{1}{T}\int_{-\infty}^{+\infty}(A_i \sin(\omega t))^2 dt = \frac{A_i^2}{2} \tag{8}$$

where A_i is the modal vibration amplitude, which can be obtained by Eq. (9)

$$A_i = \sqrt{2}\sigma_{Ai} \tag{9}$$

Considering the damper and sag effect of stay cables, the real modal shape is a little different from sinusoidal curves. To obtain real modal shape, FEM model analysis was carried out with 30 beam elements and a spring element to simulate the stay cable and the damper respectively. The free ends of each stay cable and damper were fixed. The modal shapes of stay cables could be calculated, as denoted by $\phi_i(x)$ where *i* denotes the vibration mode order and x is coordinate in chord direction. The relationship between the modal amplitude at the point of accelerometer and the maximum modal amplitude of stay cable can be shown in Fig. 15. The maximum modal amplitude of stay cable can be obtained by Eq. (10).

$$A_{\max,i} = A_i \times \frac{max(\phi_i)}{\phi_i(x_a)} \tag{10}$$

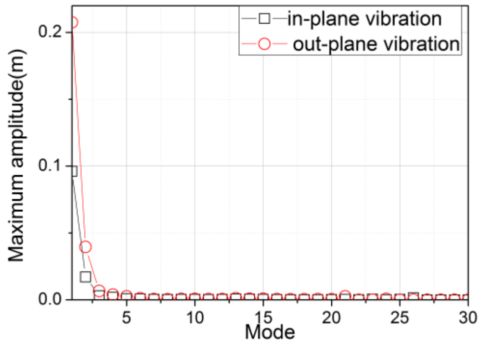

Fig. 16 Maximum averaged modal amplitude

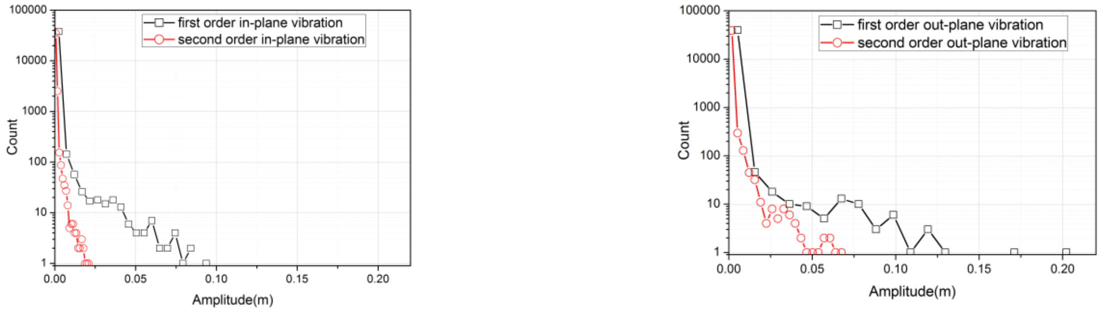

(a) in-plane vibration (b) out-plane vibration

Fig. 17 Occurrence probability of maximum average modal amplitude

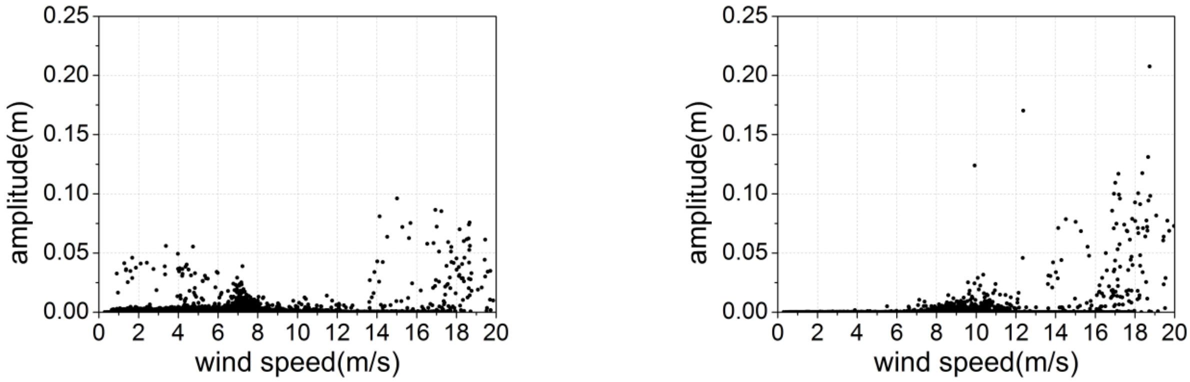

(a) in-plane (b) out-plane

Fig. 18 First order modal amplitude of SR34 vs. averaged wind speed

Table 4 Modal amplitude thresholds at different probability (unit: m)

Occurrence probability		10^{-2}	10^{-3}	10^{-4}	10^{-5}
in-plane	first mode	0.006	0.046	0.085	0.097
	second mode	0.002	0.009	0.018	0.025
out-plane	first mode	0.003	0.071	0.130	0.204
	second mode	0.001	0.024	0.052	0.083

The longest cable of SR34 was investigated by using the method mentioned above. The modal vibration amplitudes, as a function of the mode of vibration, are plotted in Fig. 16. Table 3 shows that in-plane vibration amplitudes are less than 0.1m no matter the vibration mode number. A probability of 0.003% of the out-plane vibration amplitudes exceed 0.2 m. From Table 4, the probability of 0.01% could be used as a warning of a risk of damage to the stay cable. For SR34, if an in-plane vibration amplitude is larger than 0.085 m, or an out-plane vibration amplitude exceeds 0.13 m, some inspection work should be conducted on the stay cable or its damper.

Fig. 17 gives the frequency count of amplitude of the first two modal vibration in two directions. For the first mode, the maximum average in-plane amplitude reached 0.096 m while the maximum average out-plane amplitude was about 0.21 m. Comparing in-plane vibrations with out-plane vibrations, it is clear that out-plane vibration is much stronger than in-plane vibration for stay cable SR34. For those modes higher than the third, the amplitudes become negligible.

As shown in Fig. 17, the larger the amplitude, the lower its probability of occurrence. Regardless of the direction of the vibration, or its mode, the average amplitude was less than 0.05 m for most of the year.

To further reveal the relationship between the vibration amplitude and wind speed, correlation analysis was carried out to give the first modal vibration amplitude values in 10-minute averaged wind speeds, as seen in Figs. 18 and 19.

It can be seen that two cables perform differently in a windy environment. For in-plane vibration, wind speeds of less than 8 m/s, and higher than 13 m/s, could lead to cable SR34 reaching a large vibrational amplitude, while SB18's amplitude was comparatively larger when the wind speed

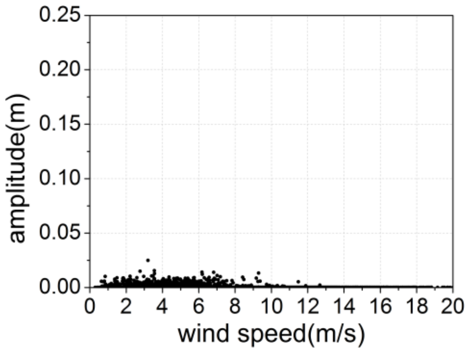

(a) in-plane

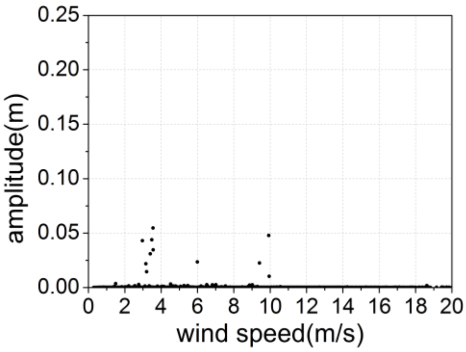

(b) out-plane

Fig. 19 First order modal amplitude of SB18 vs. averaged wind speed

was less than 10 m/s. As for out-plane vibrations, in SR34, the higher the wind speed, the more likely its vibration amplitude to increase; but, for SB18, as for out-plane motion, only wind speeds of less than 10 m/s can induce larger amplitude vibrations.

6. Conclusions

This paper has introduced the long-term monitoring of super-long stay cables on Sutong Bridge, which has provided a wealth of data detailing the wind and dynamic response characteristics of stay cables. To identify the base frequency of stay cables automatically, a new least squares method is proposed. The following conclusions can be drawn:

1) By a combination of short-term, medium-term, and long-term data analysis, and consideration of the corresponding weather conditions, an approximate wind-rain-induced vibration mode is discerned;

2) The type of vibration in the in-plane and out-plane directions is revealed. Medium-length cables mainly suffered from in-plane vibration, while for long cables, two types of vibrations can be discerned with one dominated by in-plane vibration and the other by out-plane vibration. The probability of occurrence of the two types of vibration is also calculated.

3) In normal working conditions, stay cable vibration energy focusses on frequencies of between 2 Hz and 6 Hz, while under strong wind, the vibration energy is distributed more broadly over the frequency domain, especially for in-plane vibrations at a frequency of less than 1 Hz, which may lead to significant changes in stay-cable tension force and cable vibration amplitude.

4) From the correlation analysis between vibration and wind speed, long cables are more vulnerable to high wind speeds while medium-length cables are likely to vibrate at relatively larger amplitudes at lower wind speeds.

5) The distributions of tension force and vibration amplitude are acquired from the analysis of the monitoring data. Based on the probabilities deduced therefrom, some thresholds for tension force and vibration amplitude are suggested as alarm levels to be used in the management and maintenance of stay cables and dampers.

Acknowledgments

The work described in this paper was financially supported by National Natural Science Foundation of China (Grant No. 51678437) and Guizhou Science and Technology Major Project (Contract No. [2016]3013).

References

Chen, C.C., Wu, W.H., Leu, M.R. and Lai, G. (2016), “Tension determination of stay cable or external tendon with complicated constraints using multiple vibration measurements”, *Measurement*., **86**, 182-195.

Conde, B., Del Pozo, S., Riveiro, B. and González-Aguilera, D. (2016), “Automatic mapping of moisture affectation in exposed concrete structures by fusing different wavelength remote sensors”, *Struct. Control Health Monit*., **23**(6), 923-937.

Deng, Y., Liu, Y., Feng, D. and Li, A. (2015), “Investigation of fatigue performance of welded details in long-span steel bridges using long-term monitoring strain data”, *Struct. Control Health Monit*., **22**(11), 1343-1358.

Dworakowski, Z., Kohut, P., Gallina, A., Holak, K. and Uhl, T. (2016), “Vision-based algorithms for damage detection and localization in structural health monitoring”, *Struct. Control Health Monit*., **23**(1), 35-50.

Fan, S., Ren, L. and Chen, J. (2015), “Investigation of fiber Bragg grating strain sensor in dynamic tests of small-scale dam model”, *Struct. Control Health Monit*., **22**(10), 1282-1293.

Feng, D., Scarangello, T., Feng, M.Q. and Ye, Q. (2017), "Cable tension force estimate using novel noncontact vision-based sensor", *Measurement*., **99**, 44-52.

Follen, C.W., Sanayei, M., Brenner, B.R. and Vogel, R.M. (2014), “Statistical bridge signatures”, *J. Bridge Eng*., **19**(7).

Hikami, Y. and Shiraishi, N. (1988), “Rain-wind induced vibrations of cables stayed bridges”, *J. Wind Eng. Ind. Aerod*., **29**(1-3), 409-418.

Kudva, J.N. (1994), “Design requirements and system payoffs for an on-board structural health monitoring system (SHMS)”, Proceedings of SPIE - The International Society for Optical Engineering., 2191 168-175.

Lu, P. (2008), “A statistical based damage detection approach for highway bridge structural health monitoring”, Dissertations & Theses - Gradworks.

Macdonald, J.H.G. (2016), “Multi-modal vibration amplitudes of taut inclined cables due to direct and/or parametric excitation”, *J. Sound Vib*., **363**, 473-494.

Main, J.A. and Jones, N.P. (1999), “Full-scale measurements of stay cable vibration", *Proceedings of the 10th International Conference on Wind Engineering*.

Mao, Z. and Todd, M. (2010), "A structural transmissibility measurements-based approach for system damage detection", Proceedings of SPIE - The International Society for Optical Engineering..

Matsumoto, M., Yagi, T., Shigemura, Y. and Tsushima, D. (2001), "Vortex-induced cable vibration of cable-stayed bridges at high reduced wind velocity", *J. Wind Eng. Ind. Aerod*., **89**(7), 633-647.

Raftoyiannis, I.G. and Michaltsos, G.T. (2016), "Movable anchorage systems for vibration control of stay cables in bridges", *Eng. Struct*., **112**(3), 162-171.

Sardesai, M.V. and Desai, A.K. (2014), "Free and forced vibration analysis of extradosed bridge", *Int. J. Current Res. Rev*., **6**(20), 1-10.

Schemmann, A.G. and Smith, H.A. (2015), "Vibration control of cable - stayed bridges—part 1: modeling issues", *Earthq. Eng. Struct. D*., **27**(8), 811-824.

Stallings, J.M. and Frank, K.H. (1991), "Stay-cable fatigue behavior", *J. Struct. Eng.*, 1**17**(117), 936-950.

Sun, C., Zhao, Y., Wang, Z. and Peng, J. (2015), "Effects of longitudinal girder vibration on non-linear cable responses in cable-stayed bridges", *Eur. J. Environ. Civil Eng*., 1-14.

Wang, L., Li, A., Ma, X. and Ding, S. (2012), "Stay-cable maintenance and replacement strategy based on lifetime functions", *China Civil Eng. J*., **45**(6), 162-170.

Wang, Y., Li, Z.X. and Li, A.Q. (2010), "Combined use of SHMS and finite element strain data for assessing the fatigue reliability index of girder components in long-span cable-stayed bridge", *Theor. Appl. Fract. Mech*., **54**(2), 127-136.

Wu, W.H., Wang, S.W., Chen, C.C. and Lai, G. (2016), "Application of stochastic subspace identification for stay cables with an alternative stabilization diagram and hierarchical sifting process", *Struct. Control Health Monit*., **23**(9), 1194-1213.

Zhang, Q. and Peil, U. (1999), "Dynamic behaviours of cables in parametrically unstable zones", *Comput. Struct*., **73**(1-5), 437-443.

Zuo, D., Jones, N.P. and Main, J.A. (2008), "Field observation of vortex- and rain-wind-induced stay-cable vibrations in a three-dimensional environment", *J. Wind Eng. Ind. Aerod*., **96**(6-7), 1124-1133.

CC